ISSN(Online) : 2319-8753
ISSN (Print) : 2347-6710

International Journal of Innovative Research in Science, Engineering and Technology

(An ISO 3297: 2007 Certified Organization)

Vol. 5, Issue 10, October 2016

Noise Reduction of Multi-Channel images by Low Rank Matrix Decomposition with Intensity Gradient Vector

Mohammed Aslam[1], K Jhansi Rani[2]

P.G. Student, Department of Electronics and Communication Engineering, University College of Engineering, JNTU Kakinada, Andhra Pradesh, India[1]

Assistant Professor, Department of Electronics and Communication Engineering, University College of Engineering, JNTU Kakinada, Andhra Pradesh, India[2]

ABSTRACT: Image denoising is one of the basic problems in low level vision.Reduction of noise and enhancing the images were in spatial domain increases the scope of information in the image. Then, noise and aliasing artifacts are removed from the structured matrix by applying sparse and low rank matrix decomposition technique. These also helps in reducing the non-linear artifacts. That is sparsity of the image. Nevertheless, noise amplification and aliasing artifacts are serious in pMRI reconstructed images at high accelerations. Here a low rank matrix decomposition helps in denoising the medical images using ADMM Algorithm, but was not very much efficient in reducing the error rate. So, redundant multi-resolution decomposition helps in increasing the information levels of the image. And those values were shown using performance parameters peak signal noise rate (PSNR) and structural similarity index matrix (SSIM) and entropy i.e, information of an image. And for better accuracy in the pMRI reconstructed images we introduce the method of continuous convolution process i.e, using intensity gradient vectors. The problem of getting an appropriate absolute gradient magnitude for edges lies in the method used. The Sobel operator performs a 2-D spatial gradient measurement on images. Transferring a 2-D pixel array into statistically uncorrelated data set enhances the removal of redundant data, as a result, reduction of the amount of data is required to represent a digital image.

KEYWORDS: Denoising, low rank, matrix decomposition, multi-channel coil, parallel MRI (pMRI), Sobel operator, image gradient.

I. INTRODUCTION

MRI is a extensively used diagnostic tool, that gives unmatched propensity to image soft tissue. Denoising in resonance imaging (MRI) may well be a important issue and very important for clinical identification and computerized analysis. Parallel imaging is a robust method for accelerating the acquisition of magnetic resonance imaging (MRI) data, and has made possible many new applications of MR imaging.Increasing the robustness of magnetic fields can improve the signal-noise-ratio (SNR)[10][11], but will introduce radio frequency-inhomogeneity artifacts and demand high costs as a results of the noise attenuation wants high power supply devices to rise the super conduction effect t[1]. employing a multi-channel coil array to simultaneously receive MR k-space (i.e., the spatial Fourier work on domain of imaging object) signals shows vital SNR gain. Moreover, further k-space info from these coils is employed to fill uniformly under sampled k-space by utilizing parallel tomography (pMRI) techniques which can shorten MR scanning time. Even so, noise amplification and aliasing artifacts are serious in pMRI reconstructed image at high under sampling parameters [2].

Recently, low-rank matrix completion derived from compressed sensing theory has been successfully applied to various matrix completion issues, e.g., image compression[12], video denoising and dynamic tomography [6][13].

ISSN(Online) : 2319-8753
ISSN (Print) : 2347-6710

International Journal of Innovative Research in Science, Engineering and Technology

(An ISO 3297: 2007 Certified Organization)

Vol. 5, Issue 10, October 2016

Compared with classical denoising strategies, denoising strategies based on low rank completion enforce fewer external assumptions on noise distribution. These strategies rely on the self-similarity of 3 dimensions (3-D) images across completely different slices or frames to construct a low rank matrix.
In this paper, we propose to remove both noise and aliasing artifacts in pMRI image by employing a sparse and low rank decomposition technique. By employing the self-similarity between multi-channel coil images and within themselves, we formulated the denoising of pMRI image as a non-smooth convex optimization problem that minimizes a combination of nuclear norm and l_1-norm. The proposed problem is efficiently solved by using the alternating direction technique of multipliers (ADMM) [7]. Experimental results of phantom and in vivo brain imaging are provided to authenticate the performance of the proposed technique, with comparisons to the related denoising strategies.

II. RELATED WORK

A. *SELF-SIMILARITY IN MULTI-CHANNEL COIL IMAGES*

When associate L-channel coil array is employed to receive MRk-space signals with Nyquistsampling rate, L coil images with-out aliasing artifacts are often obtained by one by one applying a 2-D inverse discrete Fourier transform on the k-space of every channel coil. Each individual coil image, s_l, are often written as a point-wise product of coil sensitivity m_l and spin density c.

$$s_l = m_l c + n_l \tag{1}$$

For $l = \{1,\ldots,L\}$, n_l is that the complex-valued noise of the lth coil. Generally, the coil sensitivity m is spatially smoothvarying within the entire field-of-view (FOV), that ends up in extended similarity among coil pictures. for every coil picture s_l, consider one image patch $p_{i,l}$ of size M×M focused at pixel i.Because the coil sensitivity are often approximated as a constant $m_{i,l}$ at intervals the patch $p_{i,l}$, image patches at pixel i across all coils, $\{p_{i,l}\}^{L}_{l=1}$, have the subsequent relationship:

$$\frac{p_{i,l}}{m_{i,l}} = \cdots = \frac{p_{i,l}}{m_{i,l}} = \cdots = \frac{p_{i,L}}{m_{i,L}} = p'_i \tag{2}$$

Where p'_i denotes the patch centered at pixel i from the originalimage c. Eq. (2) proposes all the vectors of image patches at the identical region over coils are linearly correlated. In fact, the self-similarity also exists in neighboring pixels or patches withineach coil image [8]. The similarity metric is defined as thel_2-norm of pixel value distinction between two patches. Suppose K matched patches $\{p_{i,l,k}\}_{k=1}^{K}$ are found for the processed patch $p_{i,l}$, an $M^2 \times K$ patch matrix P can be constructed by summing all these matched image patches

$$P = (p_{i,l,1}, p_{i,l,2}, \ldots, p_{i,l,K}). \tag{3}$$

Matrix P during which most columns are linearly correlated should be low rank within the absence of noise and artifacts. Nevertheless, the perturbation of noise or artifacts would increase the rank of P. Consequently, recovering a clear image from noisy coil images can be formulated as a low rank decomposition problem.

B. *DENOISING IN PMRI BY LOW RANK MATRIX DECOMPOSITION*

To remove noise and aliasing artifacts at the same time, we approximately model the image of pMRI as a superposition of clear image, aliasing artifacts and noise. Thus, every matched patch matrix P from pMRI reconstructed coil images are often decomposed as

$$P = C + D + N \tag{4}$$

Where matrix C represents the original noise-free image, which is low rank because of the self-similarity of multi-channel coil images. Matrix D symbolizes residual aliasing artifacts and has a sparse structure, matrix N signalizes

ISSN(Online) : 2319-8753
ISSN (Print) : 2347-6710

International Journal of Innovative Research in Science, Engineering and Technology

(An ISO 3297: 2007 Certified Organization)

Vol. 5, Issue 10, October 2016

random image noise that is generally introduced within the acquisition section and amplified in the pMRI reconstruction method. Because the self-similarity and sparseness can be, severally characterized by means of rank and $l_0$norm, denoising of coil images are often described as a matrix decomposition problem that extracts the clear image C from the observed image P by solving the following minimization problem:

$$\min_{C,D} rank(C) + \lambda ||D||_0$$
$$\text{s.t } \| P - C - D \|_F \leq \delta \quad (5)$$

Where $\| \|_0$ denotes l_0 norm that accounts the number of non-zero entries in matrix or vector, $\| \|_F$ states Frobenius norm for matrix, $\lambda>0$ is a tuning parameter providing a trade-off between sparse and low-rank components, and δ reflects the level of noise in observation P. Generalizations of (5) are usually intractable as a result of rank and l_0 norm arenon convex functions, we instead contemplate a convex relaxation of (5), that has also been proven to promote low-rank solutions

$$\min_{C,D} ||C||_* + \lambda ||D||_1$$
$$\text{s.t. } \| P - C - D \|_F \leq \delta \quad (6)$$

Where$\|C\|_*$ symbolizes the nuclear norm of matrix C (i.e., the sum of its singular values), and $\| \|_1$ is that the summation of $l_1$norms over all matrix columns. Eq. (6) will be resolved with as efficient ADMM method by taking full advantage ofits separate structure, that is elaborate within the following segment.

C. *OPTIMIZATION ALGORITHM*

In this paper, we tend to introduce the augmented Lagrange alternating direction methodology (ADMM) [7] for resolution non-smooth convex optimization problem(6). The augmented Lagrange function of (6) is outlined as

$$L_A(C, D, Z) = \lambda ||D||_1 + ||C||_* - [Z, C + D - P] + \beta/2 ||C + D - P||_F^2 \quad (7)$$

Where$\beta>0$ is that the penalty parameter for the violation of the linear constraint and Z is that the Lagrange multiplier factor of the linear constraint, and (.) denotes the standard trace inner product operator. The minimization task (7) will be split into 3 easier sub problems as follows

$$\begin{cases} D^{k+1} \in \text{argmin}\{L(D, C^k, Z^k)\} \\ C^{k+1} \in \arg\min\{L(D^{k+1}, C, Z^k)\} \\ Z^{k+1} = Z^k - \gamma\beta(D^{k+1} + C^{k+1} - P) \end{cases} \quad (8)$$

Algorithm 1 ADMM for Solving Sparse and Low Rank Matrix Decomposition Problem
Do

1. Compute D^{k+1}
   $D^{k+1} = (1/\beta)Z^k - C^k + P - T_{\Omega_\infty^{\lambda/\beta}}[(1/\beta)Z^k - C^k + P]$
   Where $T_{\Omega_\infty^{\lambda/\beta}}$ denotes the Euclidean projection onto
   $\Omega_\infty^{\lambda/\beta}$: $\{X \in \mathcal{H}^{nxn} | - \lambda/\beta \leq x_{i,j} \leq \lambda/\beta\}$
2. Compute C^{k+1}
   $C^{k+1} = U^{k+1}\text{diag}(\max\{\sigma_i^{k+1} - \frac{1}{\beta}, 0\})(V^{k+1})^T$
   Where U^{k+1}, V^{k+1}, and $\{\sigma^{k+1}\}$ generated by the singular values decomposition of $P - D^{k+1} + (1/\beta)Z^k$
3. Update the Z^{k+1}
   $Z^{k+1} = Z^k - \gamma\beta (D^{k+1} + C^{k+1} - P)$, $\gamma \in (0, (\sqrt{5} + 1)/2$ until converged

ISSN(Online) : 2319-8753
ISSN (Print) : 2347-6710

International Journal of Innovative Research in Science, Engineering and Technology

(An ISO 3297: 2007 Certified Organization)

Vol. 5, Issue 10, October 2016

Where $\gamma \in (0, (\sqrt{5}+1)/2)$ could be a relaxation factor to ensure convergence of iterations. The variables C, D, and Z are minimized on an individual basis, and each of them has a closed-form solution. The detail procedure for solving the problem (8) is introduced in Algorithm 1.

D. ***CONTINUOUS CONVOLUTION PROCESS***

An image gradient is a directional change in the intensity or colour in an image. Image gradients may be used to extract information from images.In graphics software for digital image editing, the term gradient or colour gradient is used for a gradual blend of colour which can be considered as an even gradation from low to high values, as used from white to black in the images to the right. Another name for this is colour progression.Mathematically, the gradient of a two-variable function (here the image intensity function) at each image point is a 2D vectorwith the components given by the derivatives in the horizontal and vertical directions. At each image point, the gradient vector points in the direction of largest possible intensity increase, and the length of the gradient vector corresponds to the rate of change in that direction.
Since the intensity function of a digital image is only known at discrete points, derivatives of this function cannot be defined unless we assume that there is an underlying continuous intensity function which has been sampled at the image points. With some additional assumptions, the derivative of the continuous intensity function can be computed as a function on the sampled intensity function, i.e., the digital image. Approximations of these derivative functions can be defined at varying degrees of accuracy. The most common way to approximate the image gradient is to convolve an image with a kernel, such as the Sobel operator or Prewitt operator.The gradient of the image is one of the fundamental building blocks in image processing. One of the most common uses is in edge detection. After gradient images have been computed, pixels with large gradient values become possible edge pixels. The pixels with the largest gradient values in the direction of the gradient become edge pixels, and edges may be traced in the direction perpendicular to the gradient direction. One example of an edge detection algorithm that uses gradients is the Canny edge detector.

The gradient of an image is given by the formula:

$$\nabla f = \begin{bmatrix} g_x \\ g_y \end{bmatrix} = \begin{bmatrix} \frac{df}{dx} \\ \frac{df}{dy} \end{bmatrix}$$

Where $\frac{df}{dx}$ is the gradient in x direction

$\frac{df}{dy}$is the gradient in y direction

The gradient direction can be calculated by the formula:

$$\theta = \tan^{-1}\left[\frac{g_y}{g_x}\right].$$

The Sobel operator is an example of the gradient method. The Sobel operator is a discrete differentiation operator, computing an approximation of the gradient of the image intensity function (Sobel& Feldman, 1968). The Sobel edge operator masks are given as

ISSN(Online) : 2319-8753
ISSN (Print) : 2347-6710

International Journal of Innovative Research in Science, Engineering and Technology

(An ISO 3297: 2007 Certified Organization)

Vol. 5, Issue 10, October 2016

-1	0	+1
-2	0	+2
-1	0	+1

Gx

+1	+2	+1
0	0	0
-1	-2	-1

Gy

The operator calculates the gradient of the image intensity at each point, giving the direction of the largest possible increase from light to dark and the rate of change in that direction.At each image point, the gradient vector points to the direction of largest possible intensity increase, and the length of the gradient vector corresponds to the rate of change in that direction. This implies that the result of the Sobel operator at any image point which is in a region of constant image intensity is a zero vector and at a point on an edge is a vector which points across the edge, from darker to brighter values.
The Sobel operator is based on convolving the image with a small, separable, and integer valued filter in horizontal and vertical direction and is therefore relatively inexpensive in terms of computations. On the other hand, the gradient approximation which it produces is relatively crude, in particular for high frequency variations in the image.

III. EXPERIMENTAL RESULTS AND DISCUSSIONS

A. *SOURCE DATA*

Noisy images were generated from the undersampled k-space data with generalized auto-calibrating partially parallel acquisitions (GRAPPA) that's the most widely used pMRI reconstruction technique in commercial MR scanners. Images reconstructed with full k-space data were used as the pseudo ground truths.

B. *ALGORITHM IMPLEMENTATION*

For the proposed methodology, the parameter λ was set following : $\lambda = 1/\sqrt{max(M^2, K)}$. The parameter β was through empirical observation set to $0.25M^2K/\sigma\|P\|_1$ for convenience, where $\sigma = \text{mode}(\sigma_p)$ is that the local standard deviation for every group of matching image patches. The relaxation factor γ was set to 1.6 for the change of Lagrange multiplier factor. To ensure the convergence of the proposed algorithm, the relative amendment at every iteration was calculated

$$\xi = \frac{\|(D^{k+1}, C^{k+1}) - (D^k, C^k)\|}{\|(D^k, C^k)\|_F + 1}$$

C. *QUALITY MEASURES*

Two quality measures were used for quantitatively conceiving the accuracy of denoised results. The primary is that the Peak signal noise rate (PSNR) metric, which is formed by calculating the ratio between the maximum possible power of a signal and the power of corrupting noise that affects the fidelity of its representation

$$\text{PSNR} = 20 \log_{10} \frac{\max(I^{ref})}{\|I^{recon} - I^{ref}\|_2}$$

ISSN(Online) : 2319-8753
ISSN (Print) : 2347-6710

International Journal of Innovative Research in Science, Engineering and Technology

(An ISO 3297: 2007 Certified Organization)

Vol. 5, Issue 10, October 2016

Where I^{recon} and I^{ref} correspondsdenoised image and noiseless reference image, severally.Another quality measure was the structural similarity index matrix (SSIM) that higher relates to the human visual system than conventional metrics supported the mean square error. The SSIM between two images I and J is given by

$$SSIM(I,J) = \frac{1}{N}\sum_{i\varepsilon I, j\varepsilon J} \frac{(2\mu_i\hat{\mu}_j+c_1)(2\sigma_{i,j}+c_2)}{(\mu_i^2+\hat{\mu}_j^2+c_1)(\sigma_i^2+\sigma_j^2+c_2)}$$

Where μ_i and $\hat{}\mu_j$ are the various local mean values, σ_i and σ_j the respective standard deviations, $\sigma_{i,j}$covariance value, $c_1$and c_2 two predefined constants. The higher PSNR and SSIM indicate more preferred image quality.

D. ***RESULTS***

The Sobel operator performs a 2-D spatial gradient measurement on an image. Typically, it is used to find the approximate absolute gradient magnitude at each point I of an input grayscale image. The Sobel edge detector uses a pair of 3 x 3 convolution masks, one estimating gradient in the x-direction and the other estimating gradient in y-direction. A convolution is usually much smaller than the actual image. As a result, the mask is slide over the image manipulating a square of pixels at a time. It is important to note that pixels in the first row and last row, as well as the first and last column cannot be manipulated by a 3 x 3 mask. The zoomed-in patches shows the residual artifacts are retained in the filtered pictures of LMMSE, BM4-D, and ANLM. In contrast, each noise and residual artifacts are removed within the denoised image by the proposed methodology at a little sacrifice of image contrast. Note that the noise within the background region of LMMSE denoised image is amplified. This is because the standard deviation of noise is automatically approximated in LMMSE according to the background noise, that ignores the spatially varied noise. Fig. 1(a), 1(b), 1(c) shows original, noise and denoised image of sagittal brain MRI images. Fig. 2(a), 2(b), 2(c) shows original, noise and denoised image of axial brain MRI images.

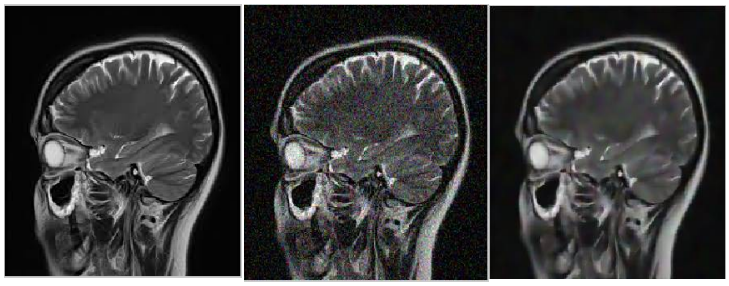

(a) (b) (c)

Fig. 1(a) Original Image, 1(b) Nosie Image, 1(c) denoised image of Sagittal Brain.

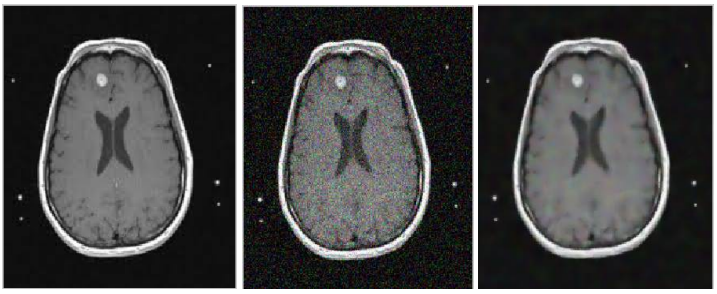

(a) (b) (c)

Fig. 2(a) Original Image, 2(b) Nosie Image, 2(c) denoised image of Axial Brain.

ISSN(Online) : 2319-8753
ISSN (Print) : 2347-6710

International Journal of Innovative Research in Science, Engineering and Technology

(An ISO 3297: 2007 Certified Organization)

Vol. 5, Issue 10, October 2016

TABLE - I

Image	LMMSE	BM4D	Proposed
Axial			
PSNR	41.127	46.327	47.6823
SSIM	0.9258	0.9467	0.9843
Sagittal			
PSNR	24.929	26.9731	28.3890
SSIM	0.7926	0.9126	0.9521

The local images zoomed in and listed within the left-bottom of the denoised images, severally. The zoomed in patch shows ANLM has a lot of conservative behavior on noise suppression than BM4-D and therefore the proposed methodology.

Although the image filtered by the proposed methodology seems to be slightly over smoothed, the zoomed-in patch image shows the proposed methodology preserves most of the important features in the filtered image. The noise level in the image of LMMSE is slightly higher than other results. The aliasing artifacts are weaker within the image denoised by the proposed methodology than those of LMMSE and BM4-D.

Results of quantitative evaluation of PSNR and SSIM values are reported in Table- I for different methods. As shown, the proposed methodology outperforms alternative approaches in all cases. LMMSE that was directly applied on single noisy image has the shortest denoising time. The proposed methodology has the longest time among all denoising methods; however, it can still meet the real-time necessities in clinical applications by employing the proposed algorithmin C programing language.

Edges play quite an important role in many applications of image processing, in particular for machine vision systems that analyze scenes of man-made objects under controlled illumination conditions. Detecting edges of an image represents significantly reduction the amount of data and filters out useless information, while preserving the important structural properties in an image.

IV. CONCLUSION

We have represented a unique denoising methodology for pMRI by exploiting the self-similarity between multi-channel coil images and within themselves. The planned methodology simultaneously removes noise and aliasing artifacts by leveraging sparse and low rank matrix factorization.

The Sobel operator performs a 2-D spatial gradient measurement on an image. Typically it is used to find the approximate absolute gradient magnitude at each point I of an input grayscale image. The Sobel edge detector uses a pair of 3 x 3 convolution masks, one estimating gradient in the x-direction and the other estimating gradient in y–direction. It is easy to implement than the other operators.Although the Sobel operator is slower to compute, it's larger convolution kernel smoothes the input image to a greater extent and so makes the operator less sensitive to noise.

Sobel operator effectively highlights noise found in real world images as edges though, the detected edges could be thick.Experimental results demonstrate that the proposed algorithm can benefit each visual diagnostic and quantitative methodologies. The proposed method may be extended to multiple dimensions imaging by exploiting the redundancy and uniformity between multi-slice and multi-frame images to attain a better SNR gain that's warranted during a future study.This method can be applied to other bio-medical images (Retina, Face) also for noise reduction.

ISSN(Online) : 2319-8753
ISSN (Print) : 2347-6710

International Journal of Innovative Research in Science, Engineering and Technology

(An ISO 3297: 2007 Certified Organization)

Vol. 5, Issue 10, October 2016

REFERENCES

[1] H. Wada et al., "Prospect of high-field MRI," IEEE Trans. Appl. Supercond., vol. 20, no. 3, pp. 115–122, Jun. 2010.
[2] A. Deshmane, V. Gulani, M. A. Griswold, and N. Seiberlich, "Parallel MR imaging," J. Magn. Resonance Imag., vol. 36, no. 1, pp. 55–72, Jul. 2012.
[3] H. Liu, C. Yang, N. Pan, E. Song, and R. Green, "Denoising 3-D MR images by the enhanced non-local means filter for Rician noise,"Magn.ResonanceImag., vol. 28, no. 10, pp. 1485–1496, Dec. 2010.
[4] S. Aja-Fernandez, V. Brion, and A. Tristan-Vega, "Effective noise es-timation and filtering from correlated multiple-coil MR data,"Magn.ResonanceImag., vol. 31, no. 2, pp. 272–285, Feb. 2013.
[5] D. J. Larkman and R. G. Nunes, "Parallel magnetic resonance imaging,"Phys. Med. Biol., vol. 52, no. 7, pp. R15–R55, Apr. 7, 2007.
[6] S. G. Lingala, H. Yue, E. Dibella, and M. Jacob, "Accelerated dynamicMRI exploiting sparsity and low-rank structure: k-t SLR," IEEE Trans.Med. Imag., vol. 30, no. 5, pp. 1042–1054, May 2011.
[7] T. M and Y. X, "Recovering low-rank and sparse components of matrices from incomplete and noisy observations," SIAM J. Optim., vol. 21, no. 1,pp. 57–81, Jan. 2011.
[8] J. V. Manjón, P. Coupé, A. Buades, D. Louis Collins, and M. Robles, "New methods for MRI denoising based on sparseness and self-similarity," Med. Image Anal., vol. 16, no. 1, pp. 18–27, Jan. 2012.
[9] Lin Xu, Changqing Wang, Wufan Chen, Wufan Chen, Xioayun Liu, "Denoising Multi-Channel Images in Parallel MRI by Low Rank Matrix Decomposition," IEEE Trans. Applied Superconductivity., vol. 24, no. 5, Oct. 2014.
[10] www.dicomlibrary.com, www.stackoverflow.com.
[11] W. Xu and G. Hauske, "Picture quality evaluation based on error segmentation," in Proc. SPIE, vol. 2308, 1994, pp. 1454–1465.
[12] Bai ZZ, Zhang SL. A regularized conjugate gradient method for symmetricpositive definite system of linear equations. J Comput Math 2002;20:437-48.
[13] Gonzalez, R., & Woods, R. (2002). Digital image processing (2nd ed.). Prentice-Hall Inc. 567-612.
[14] Canny, J. F. (1986). A computational approach to edge detection. IEEE Trans Pattern Analysis and Machine Intelligence, 8(6), 679-698.